

Article

Impact of Cosmetic Lotions on Nanoparticle Penetration through *ex Vivo* C57BL/6 Hairless Mouse and Human Skin: A Comparison Study

Samreen Jatana ¹, Linda M. Callahan ², Alice P. Pentland ³ and Lisa A. DeLouise ^{1,3,*}

¹ Department of Biomedical Engineering, University of Rochester, Rochester, NY 14642, USA; samreen.jatana@rochester.edu

² Department of Pathology and Laboratory Medicine, University of Rochester Medical Center, Rochester, NY 14642, USA; Linda_Callahan@urmc.rochester.edu

³ Department of Dermatology, University of Rochester Medical Center, Rochester, NY 14642, USA; Alice_Pentland@urmc.rochester.edu

* Correspondence: Lisa_DeLouise@urmc.rochester.edu; Tel.: +1-585-275-1810

Academic Editor: Enzo Berardesca

Received: 14 October 2015; Accepted: 14 February 2016; Published: 19 February 2016

Abstract: Understanding the interactions of nanoparticles (NPs) with skin is important from a consumer and occupational health and safety perspective, as well as for the design of effective NP-based transdermal therapeutics. Despite intense efforts to elucidate the conditions that permit NP penetration, there remains a lack of translatable results from animal models to human skin. The objectives of this study are to investigate the impact of common skin lotions on NP penetration and to quantify penetration differences of quantum dot (QD) NPs between freshly excised human and mouse skin. QDs were mixed in seven different vehicles, including five commercial skin lotions. These were topically applied to skin using two exposure methods; a petri dish protocol and a Franz diffusion cell protocol. QD presence in the skin was quantified using Confocal Laser Scanning Microscopy. Results show that the commercial vehicles can significantly impact QD penetration in both mouse and human skin. Lotions that contain alpha hydroxyl acids (AHA) facilitated NP penetration. Lower QD signal was observed in skin studied using a Franz cell. Freshly excised human skin was also studied immediately after the sub-cutaneous fat removal process, then after 24 h rest *ex vivo*. Resting human skin 24 h prior to QD exposure significantly reduced epidermal presence. This study exemplifies how application vehicles, skin processing and the exposure protocol can affect QD penetration results and the conclusions that may be drawn between skin models.

Keywords: nanoparticles; quantum dots; skin penetration; skin lotions

1. Introduction

The expanding commercialization of products that contain engineered nanoparticles (NPs) has generated vast interest among researchers in the nanotoxicology field to better understand their fate and transport in biological systems [1–4]. Many types of NPs (e.g., silica, fullerene, carbon nanotubes, gold, silver, cerium oxide, iron oxide, quantum dots, and polymers) with altered surface chemistries have been studied [5–7]. The increasing presence of metal oxide NPs in daily wear ultra-violet radiation (UVR) protective cosmetic products has driven considerable effort to understand the conditions that may permit TiO₂ and ZnO NPs to penetrate the skin barrier [8,9]. Various *in vivo* as well as *ex vivo* skin models (rat, mouse, pig and human) have been used to examine the effects of NP physiochemical properties (e.g., size, composition, charge) and exogenous factors (e.g., UVR,

dermabrasion, tape stripping, flexion, chemical agents) on NP skin penetration, systemic translocation and toxicity [5,10–23]. Studies consistently report that healthy skin is a formidable barrier to NP penetration. Higher levels of penetration are generally observed through barrier-impaired skin [7,24]. For example, polymer particles (500 nm diameter) exhibited three-fold higher penetration in inflamed mouse skin compared to healthy controls with particular accumulation in the hair follicles and sebaceous glands [24]. Targeting NPs to hair follicles is being exploited for the development of NP-based cosmeceuticals, transdermal drug delivery and vaccination systems [14,25–32]. Gold NPs that were engineered to deliver gene silencing oligonucleotides targeting the keratinocyte epidermal growth factor receptor (EGFR) were reported to significantly reduce mouse skin thickness when topically applied mixed in Aquaphor[®], a commonly used commercial petrolatum-based skin moisturizer [33].

Despite the growing body of literature investigating NP skin interactions and NP-based transdermal drug delivery systems, the ability to use much of this information for human environmental health and safety assessment suffers from an incomplete understanding of how to translate results from animal studies to human skin. Moreover, when NPs are applied to skin mixed in lotions, the vehicle ingredients may affect NP skin penetration, a variable that is largely ignored [6,33–36]. This knowledge is especially critical for assessing occupational risk where chronic skin exposure to NPs in the work place may occur. To help elucidate these concerns, we examine the tendency of fluorescent quantum dot (QD) NPs to penetrate fresh *ex vivo* human and fresh *ex vivo* mouse skin when topically applied. We used seven vehicles, including five common commercial skin lotions and two different exposure protocols to define penetration effects.

QDs are semiconductor NPs with inherent fluorescent properties that are widely exploited in the energy and lighting industries and in biological research [37,38]. In addition to occupational exposure concerns, they are a convenient choice to study NP skin penetration given the ability to track QDs in tissue using fluorescence microscopy. In previous work using an *in vivo* mouse model we reported that QDs topically applied in a glycerol vehicle can cross the stratum corneum and that UVR exposure induces a skin barrier defect that enhances penetration and systemic distribution [19,20]. In this study we quantify the presence of QDs in the stratum corneum and in the viable epidermis using Confocal Laser Scanning Microscopy (CLSM). We exploit several advantageous features of CLSM including its high resolution imaging capability with depth selectivity to ~50 μm , optical sectioning and three-dimensional reconstruction of the acquired images [6,39]. Our studies were designed to test the effect of the QD application vehicle, the skin processing protocol and the QD skin exposure model on the QD penetration profile. Despite known architectural and biochemical differences that exist between human and mouse skin [40] that affect the percutaneous penetration of small molecular weight drugs and chemicals, our finding suggests that NP penetration trends in skin behave in a complex way that is greatly influenced by skin condition, application vehicle and method of measuring penetration.

2. Materials and Methods

2.1. Quantum Dot (QD) Functionalization

Commercially available CdSe-ZnS core/shell nanocrystals dissolved in toluene and capped with octadecyl ligands (ODA) for stability were purchased from NN Labs (5.8 nm core diameter, 600–620 nm emission peak, Fayetteville, AR, USA). Water-soluble QDs were prepared with a Glutathione (GSH) (reduced free acid Calbiochem[®]) using a ligand exchange process previously described [41]. The concentration of the sample was determined by measuring the UV-Vis absorbance on a Nanodrop spectrophotometer (Thermo Scientific, Waltham, MA, USA) at the first exciton and using Lambert-Beer's Law. The Malvern Zetasizer Nano ZS (Malvern Instruments Inc., Worcestershire, UK) was used to determine the hydrodynamic diameter (20.9 ± 1.5 nm) by light scattering and surface charge (-23.8 ± 0.7 mV) by zeta potential measurements made in distilled water (pH = 6.7) [41].

2.2. Skin Preparation

2.2.1. Mouse Skin

Skin was harvested from the back of hairless C57BL/6 mice aged 5–9 months using a stainless steel surgical blade (Miltex, Inc., Plainsboro, NJ, USA). For each experimental set-up, skin samples of about $\sim 4 \text{ cm}^2$ were cut and used directly after extraction with an intact stratum corneum, epidermis and dermis. Animal experiments were approved by the University Committee on Animal Resources (UCAR#2010-024/100360) at the University of Rochester Medical Center.

2.2.2. Human Skin

Our *ex vivo* viable human skin samples were obtained fresh from de-identified healthy adult donors following mammoplasty (Strong Memorial Hospital, Rochester, NY, USA). Usage was approved by the University of Rochester Research Subjects Review Board (RSRB00042616). Skin was used within 4 h of surgery and was stored at $4 \text{ }^\circ\text{C}$ prior to use. The skin samples were rinsed with sterile 1X phosphate buffered saline (PBS) to remove blood and debris, treated with $100 \text{ }\mu\text{L}$ fungizone (Invitrogen) in 100 mL 1X PBS for 10 min to remove pathogenic microbes, and rinsed thoroughly with 1X PBS again. A sterile surgical blade was used to remove the subcutaneous fat and to thin the dermal layer leaving the epidermis intact in order to maintain healthy tissue hydration with nutrient media for the duration of the application (24 h). The imaging was performed in the epidermis, which remained intact after the fat removal process. The thickness of the processed samples was $\sim 1.5 \text{ mm}$. Skin samples about $\sim 4 \text{ cm}^2$ in area were cut from the surgical tissue for each sample tested. In a separate test, human skin was allowed to rest for a 24 h period in serum free media (Dulbecco's Modified Eagle Medium, Gibco-Life Technologies, Waltham, MA, USA) at $37 \text{ }^\circ\text{C}$ post-processing before the topical NP application. This additional step allows the skin to recover from the blunt trauma during the fat removal process [42] that we show here can affect NP skin penetration. Although we did not test skin integrity using transepidermal water loss (TEWL) or conductivity measurements (transepithelial electrical resistance, TEER) extreme care was taken during tissue processing not to damage the stratum corneum. The samples were obtained from 4 different donors and the experiments were performed on separate days.

2.3. Ex Vivo Skin QD Exposure Experimental Protocol

Seven vehicles including 5 commercial lotions (Supplementary Data Table S1) were selected for the *ex vivo* QD penetration study including Vaseline Intensive Rescue-Clinical Therapy (Unilever, London, UK), Eucerin Plus Smoothing Essentials (Beiersdorf Inc., Wilton, CT, USA), Eucerin Everyday Protection-SPF 15 (Beiersdorf Inc.), Eucerin Calming Itch Relief (Beiersdorf Inc.), Dermovan (Healthpoint Ltd., Darwin Court, UK), Glycerol (J.T.Baker[®]) and water. Glycerol is a common ingredient in many skin care lotions [43] and it was examined in our previous work [19] so we included it in this study. Two different QD exposure protocols were used to quantify penetration through mouse and human skin; (1) Petri Dish, in which skin is placed on a hydrated cotton gauze sponge (Becton Dickinson and Company, Waltham, MA, USA) and (2) the standard Franz diffusion chamber (PermeGear Inc., Hellertown, PA, USA). For petri dish studies, the skin harvested from mice and processed human skin were placed on gauze sponge $5.1 \text{ cm} \times 5.1 \text{ cm}$ (Covidien Curity[™]) immersed in 4 mL of Dulbecco's Modified Eagle Medium (DMEM) 1X (Gibco, Life Technologies) in a polystyrene Falcon petri dish ($60 \text{ mm} \times 15 \text{ mm}$) with the air exposed epidermis facing upwards (Supplementary Figure S1). DMEM contained 10% Fetal Bovine Serum (Gibco, Life Technologies) and 1% Penicillin Streptomycin (Gibco, Life Technologies). A fixed concentration of QDs mixed with the vehicle ($0.01 \text{ mg QDs per cm}^2$ skin in 0.05 g vehicle) was applied on the stratum corneum as a uniform layer using a soft elastomer spatula. Extreme care was taken to control the area of application without contaminating the edges. Eucerin Smoothing Lotion with no QDs served as a control. The petri dishes were placed in a humidifying chamber at room temperature for the duration of the study. The samples

were photographed under a hand-held UV Lamp immediately after application and 24 h after the application. The QD intensity appeared unchanged in all the treatment groups after a 24 h exposure showing that QDs do not dissolve in the vehicles (Supplementary Figure S2). For the Franz diffusion cell study, mouse or human skin samples were placed between the donor and receptor chamber of the Franz diffusion cell using a clamp at the joint. The receptor chamber contained DMEM 1X (10% FBS, 1% Pen Strep) and a stir bar. QDs (0.01 mg per cm²) were mixed in 0.05 g of the vehicle and applied on the 1 cm² exposed area of the skin through the donor chamber (Supplementary Figure S1). Concentration of QDs mixed with the vehicle per cm² was kept consistent with the application area in the petri dish set-up. The Franz cells were placed on a stirring plate at room temperature for the duration of the experiment. At the completion of each study, the application vehicle with excess QDs was wiped off using a cotton tipped applicator (Q-tip) and the skin sample was stored at −80 °C until further analysis. The duration of each QD exposure was 24 h unless stated otherwise.

2.4. Validation of the Imaging Technique: Diffusion and Injection of QDs in *ex Vivo* Human Skin

Two different techniques were used to introduce a high concentration of QDs in human skin to validate the confocal imaging parameters. First, after fat removal, human skin (4 cm² area) was immersed in a 0.195 μM QD solution in DI water (1 mL total volume) for a duration of 22 h in a petri dish. Then 50 μL of QDs (3.9 μM) was pipetted on the epidermis and the skin was incubated for another 2 h. After the incubation, the epidermal skin surface was wiped dry using a gauze sponge and the whole tissue was imaged using Confocal Laser Scanning Microscopy (CLSM). The same skin sample was then cryo-sectioned and imaged using standard histology techniques. Second, a solution of 1.95 μM QDs in DI water (100 μL total volume) was injected into the human skin using an insulin needle. The needle was positioned into the dermis and the solution was released gradually as the syringe withdrawn towards the epidermis. The skin sample was imaged using CSLM and cryo-sectioned to obtain the side profile views.

2.5. Confocal Microscopy and Image Analysis

The set-up for CLSM is described in detail in Figure 1. Skin (~1 cm² in area) was cut out from the center of the vehicle-exposed sample and placed in a microwell dish (MatTek Corporation, Ashland, MA, USA) with the epidermis facing down for confocal imaging. The system was adjusted so negligible autofluorescence was observed at the QD emission peak (605 nm) in the control mouse and human skin samples (Supplementary Figure S3). Images obtained using CLSM were processed using ImageJ Analysis software (NIH, version 1.48). Each image (8 bit) was split into 3 channels. The red channel (QDs) was retained for analysis and the pixel information was extracted using the histogram function. A high threshold cut-off for quantifying the QD fluorescence signal was set in ImageJ between 220 and 255. The pixel number was averaged to obtain relative intensity of the QDs in each individual image between the depths of 0–40 μm. A cut off depth of 40 μm for imaging was set to quantify penetration differences (human *vs.* mouse skin) into viable epidermis, as sensitivity decreased significantly beyond this depth.

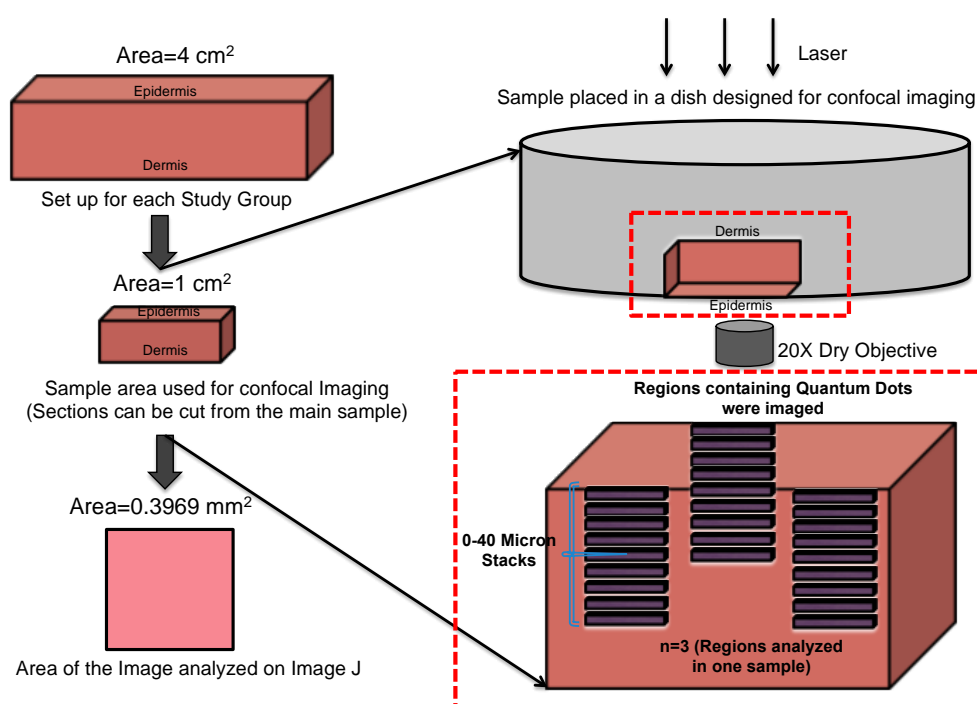


Figure 1. Schematic of Confocal Imaging set up to quantify QD penetration through *ex vivo* mouse and human skin. Skin samples from mouse and human skin (~4 cm² area) were placed in a petri dish for the 24 h study. The vehicles were applied topically and the samples were placed in a humidifying chamber. The skin samples were wiped after the 24 h incubation and processed for Confocal Laser Scanning Microscope (CLSM). Skin samples (~1 cm² area) were inverted then placed in a petri dish with a cover slip for imaging using the CLSM. Three regions containing QDs were imaged in each skin sample to a depth of 40 μ m. Images were analyzed using NIH ImageJ software.

2.6. Statistical Analysis

Data are expressed as mean \pm Standard error of the mean (SEM) and are representative of four separate experiments using different skin donors/mice unless otherwise stated ($N = 4$). A 2-tailed Student's *t*-test, unpaired with unequal variances, was used to compare penetration differences between all the commercial vehicles and water vehicle. $p < 0.05$ was considered significant. Power analysis was performed on the preliminary data obtained at the values $\alpha = 0.05$, $(1 - \beta) > 0.80$, where $(1 - \beta)$ is the statistical power of the test. The results showed that we would require at least 4 individual skin samples for each study group ($N = 4$) and 3 regions of analysis within each sample ($n = 3$). All experiments were performed on separate days, which reflect high intermediate precision in the data set obtained.

3. Results and Discussion

To investigate the effect of vehicle on QD penetration in mouse and human skin, we mixed QDs in seven different vehicles including five commercial skin lotions (Supplementary Data Table S1), glycerol (>99% purity) and water. Vehicles with QDs were topically applied immediately after processing the skin sections using the petri dish exposure protocol for 24 h. After the incubation period, residual vehicle was wiped off using Q-tips and the samples were processed for CLSM. QD presence in skin was quantified from the fluorescence image z-stacks (0–40 μ m) using NIH ImageJ software. Results (Figure 2a) show that the Eucerin smoothing lotion significantly enhanced the penetration of QDs at depths of 0, 5 and 10 μ m in *ex vivo* mouse skin compared to all other vehicles. The total fluorescence signal, integrated from 0 to 40 μ m, suggests that the QD penetration in the Eucerin smoothing lotion group was ~two-fold higher compared to water (Supplementary Figure S4a). QD penetration in the

Dermovan group was comparable to that of water. Total penetration in all other treatment groups was significantly lower ($p < 0.05$) compared to water. NP in Vaseline Intensive Care lotion also exhibited negligible QD penetration. Three-dimensional reconstruction of the image z-stacks suggests that uniform diffusion of QDs across the skin barrier does not occur (Figure 2b). Rather, as has been suggested previously, QDs appear to penetrate into the viable epidermis through high fluency entry points including defects in the stratum corneum and hair follicles [20,44]. Based on these results, we selected Eucerin smoothing lotion, Dermovan and glycerol for comparison studies using fresh *ex vivo* human skin.

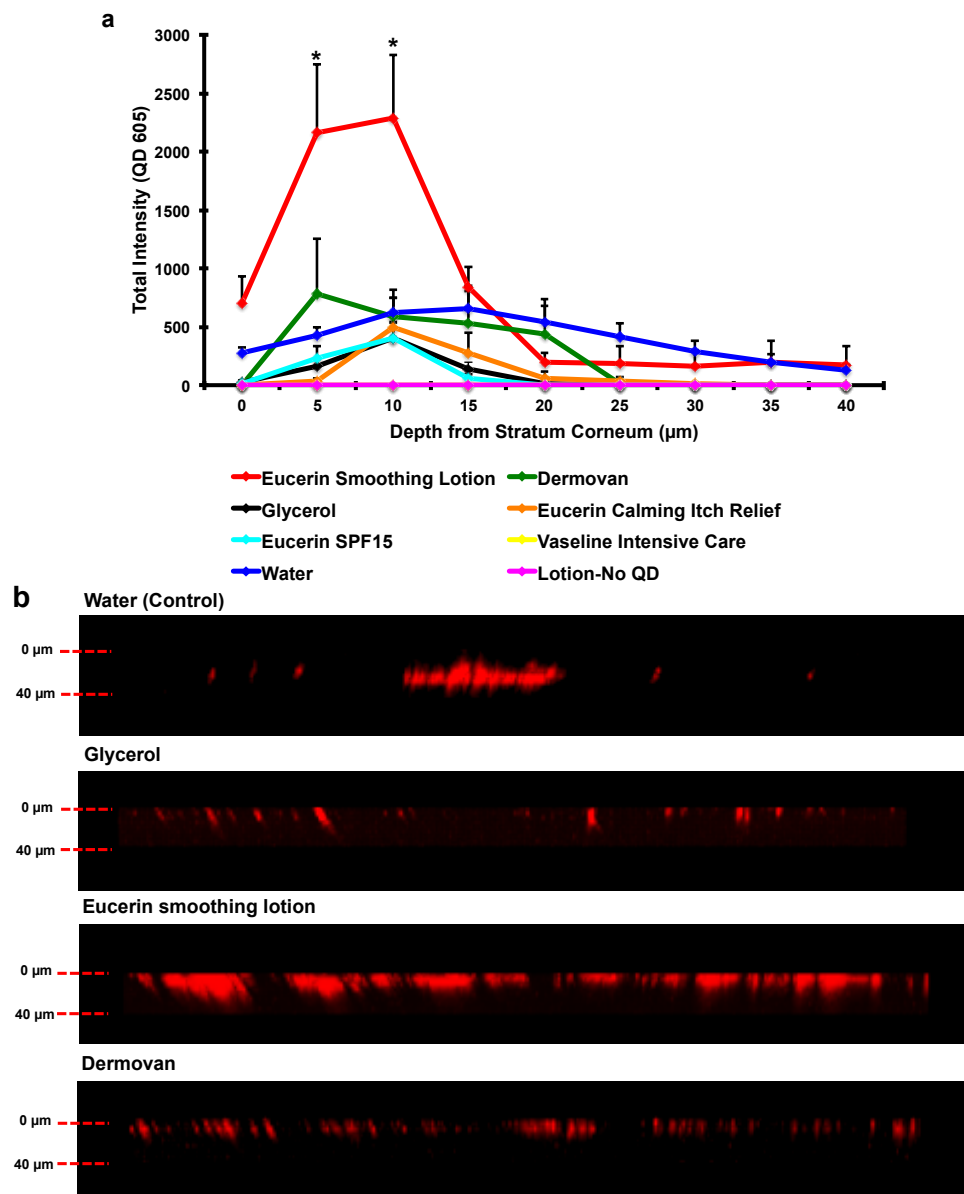


Figure 2. Eucerin Smoothing lotion enhances QD penetration through *ex vivo* mouse skin in the petri-dish protocol. (a) Significant increase in the QD presence was observed in the Eucerin smoothing lotion group at depths of 5 and 10 µm from the stratum corneum compared to water. All other vehicles exhibited QD penetration trends similar to or lower than the water treated group. Vaseline intensive care lotion exhibited negligible penetration; Mean \pm SEM ($N = 4, n = 3$); (b) three-dimensional reconstruction of the z-stacks (0–40 µm) obtained by using CLSM shows that QDs do not penetrate skin by a uniform Fickian diffusion process. QDs appear to penetrate into the viable epidermis through high fluency entry points in the stratum corneum. * $p < 0.05$ vs. water.

Studies were next conducted using the petri dish exposure protocol to investigate the effect of the 4 different vehicles on QD penetration through *ex vivo* human skin. It is important to note here that the *ex vivo* mouse skin was used, as is, post excision whereas the *ex vivo* human skin undergoes processing to remove subcutaneous fat (which can be centimeters thick when it comes from the operating room) so it is ready for QD penetration studies. Previous studies have shown that processing of freshly excised *ex vivo* human skin causes mast cell degranulation, which increases tissue vasodilation and cytokine release [42]. Resting human skin for 24 h in serum free media post-processing allowed cytokines to return to baseline values. Because vasodilation and skin inflammation could affect NP penetration we chose to compare QD penetration levels in *ex vivo* human skin <2 h and 24 h post-processing [24,45].

Results for *ex vivo* human skin exposed to QDs < 2 h post processing (Figure 3a) show vehicle-dependent penetration trends remarkably similar to that observed in the mouse skin study (Figure 2a). Significant differences in QD signals were observed at 10, 15, 30 and 35 μm in the Eucerin smoothing lotion group compared to the water control group (Figure 3a). However, comparing the QD fluorescence signal intensity observed in human skin (*y*-axis 0–8000, Figure 3a) to mouse skin (*y*-axis 0–3000, Figure 2a), the 3D z-stack reconstructions (Figure 2b *vs.* Figure 3b) suggest a much higher presence of QDs in human skin after the 24-h exposure. Taking the ratio of the integrated fluorescence intensity signal in human *versus* mouse skin reveals a 4.4-fold higher intensity for the Eucerin smoothing lotion group and 3.84 fold higher intensity signal for the water control (Supplementary Figure S4a,b). The apparent four-fold higher presence of QDs in human skin compared to mouse could be attributed to several factors including differences in the epidermal thickness between mouse (~30 μm) and human (~100 μm), which may allow faster transit completely through mouse skin or to a reduced barrier function in human skin due to processing, which may have facilitated QD penetration.

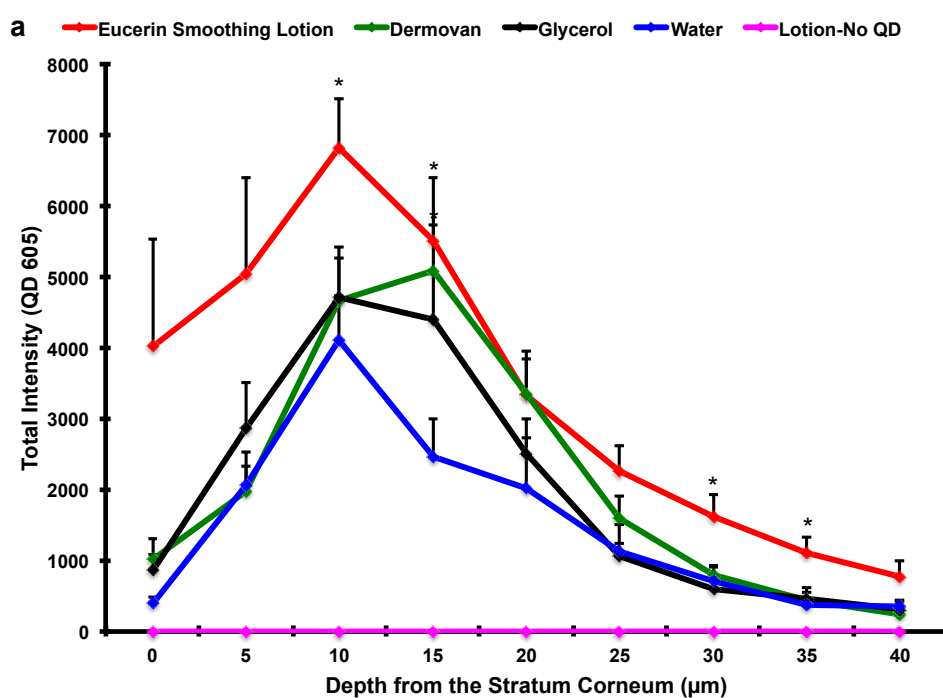


Figure 3. Cont.

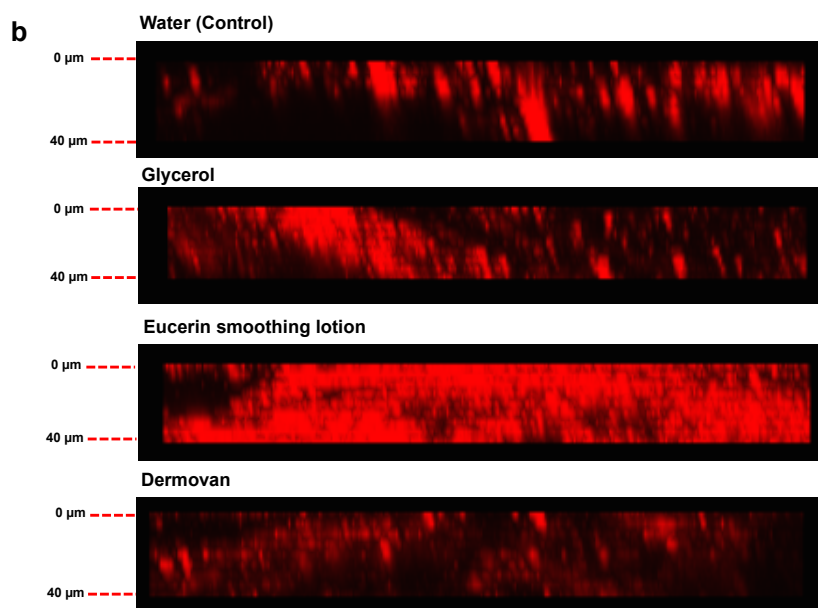


Figure 3. Eucerin Smoothing lotion enhances QD penetration through *ex vivo* human skin in the petri-dish protocol. (a) Significant increase in the QD presence was observed in the Eucerin smoothing lotion group at the depth of 10, 15, 30 and 35 μm compared to water treated group. All other vehicles exhibited QD penetration trends similar to the water; Mean \pm SEM ($N = 4, n = 3$); (b) three-dimensional reconstruction of the z-stacks (0–40 μm) obtained by using CLSM shows that QDs do not penetrate skin by a uniform Fickian diffusion process. QDs appear to penetrate into the viable epidermis through high fluency entry points in the stratum corneum. The data suggest that much more penetration is evident in human skin compared to mouse skin. * $p < 0.05$ vs. water.

To test the effect of skin processing protocol, we conducted similar penetration studies on human skin that was allowed to rest for 24 h post-processing before QD application. Results (Figure 4) showed that resting skin significantly reduced the epidermal presence of QDs for most vehicles. The ratios of the integrated QD fluorescence intensity (0–40 μm z-stacks) for the human skin (no rest) to human skin (rested 24 h) in Eucerin smoothing lotion, Dermovan and water-treated test groups were 5.5, 29.2 and 3.6, respectively (Figure 4b). This result suggests that processing the living skin tissue induces a barrier defect that enhances QD penetration. Unexpectedly, no significant differences in QD penetration were observed between the fresh processed (no rest) and rested (24 h) skin samples for the glycerol vehicle group. This likely results from the fact that glycerol is a humectant that is known to increase stratum corneum hydration and to act as a penetration enhancer [43,46]. Hence, it is plausible that the hygroscopic nature of glycerol facilitated QD penetration in both the rested and unrested skin sample (Figure 4b). More importantly, comparing the integrated QD fluorescence intensity (0–40 μm z-stacks) between mouse and rested human skin shows no significant differences were observed between the two skin types for Eucerin smoothing lotion and water (Figure 5). A statistically significant difference was seen for Dermovan with slightly higher QD presence (~three-fold) detected in the mouse skin relative to rested human skin but the magnitude of the QD presence in the rested human skin was reduced ~30-fold relative to unrested skin in the Dermovan treatment group. Over all, penetration levels for both water and Eucerin smoothing lotion in rested human and mouse skin were comparable (Figure 5).

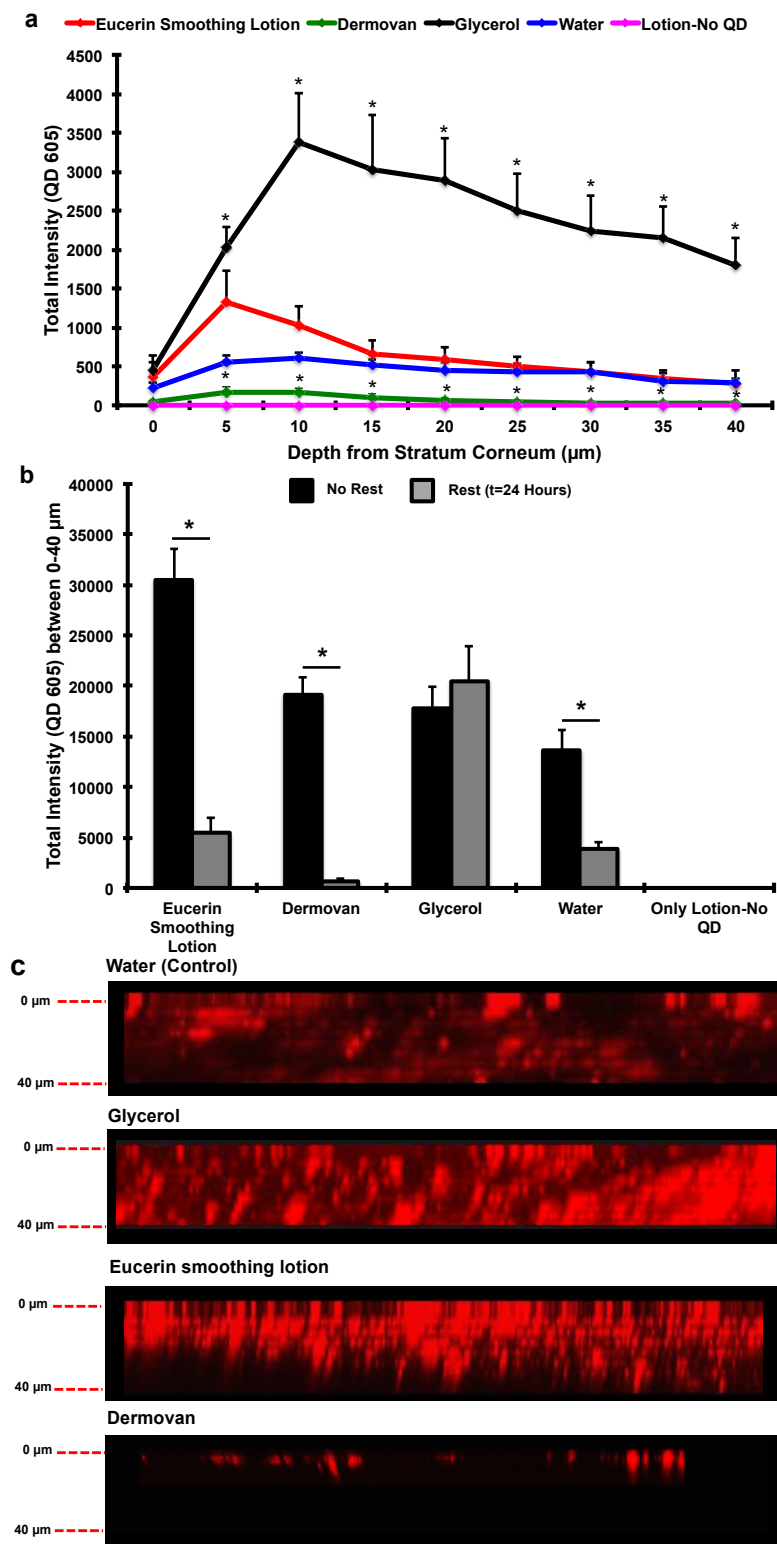


Figure 4. *Ex vivo* skin processing prior to QD application alters QD penetration in human skin. (a) QD presence in human skin rested 24 h prior to QD application was quantified using CLSM. A significant increase in QD presence was observed in the glycerol group compared to water. All other vehicles exhibited QD penetration trends similar to the water; Mean \pm SEM ($N = 4$, $n = 3$). * $p < 0.05$ vs. water; (b) comparison of integrated QD fluorescence intensity in human skin; rest vs. no rest. A significant decrease in QD presence was observed in the Eucerin smoothing lotion (5.5-fold), Dermovan (29.2-fold) and water (3.6-fold) rested skin groups compared to non-rested groups. No significant differences were observed in the glycerol group; mean \pm SEM ($N = 4$, $n = 3$). * $p < 0.05$; (c) side profile view of rested human skin showing lower presence of QDs in the Eucerin Smoothing Lotion and Dermovan treatment group compared to human skin that is not rested.

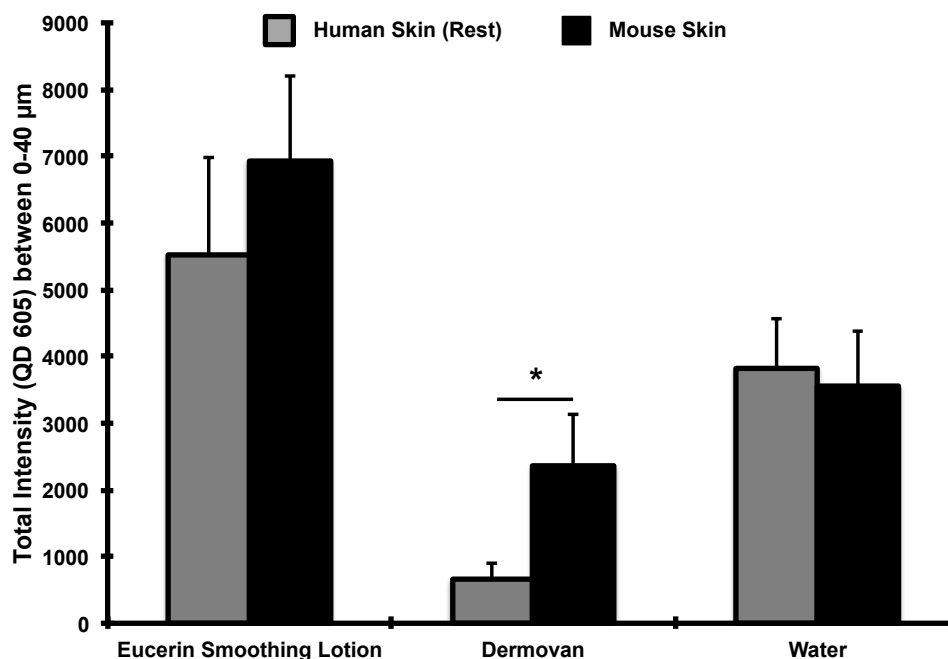


Figure 5. QD penetration trends between *ex vivo* mouse and rested human skin following a 24 h exposure using the petri dish protocol are comparable. No significant differences in the integrated QD fluorescence intensity were observed in the Eucerin smoothing lotion and water test groups between mouse skin and human skin rested for 24 h post-processing. A ~3-fold higher QD presence was observed in the Dermovan group; mean \pm SEM ($N = 4, n = 3$). * $p < 0.05$.

It is interesting to note that for both mouse and human skin we observe that the fluorescence intensity profile decays after a depth of 10–15 μm (Figures 2a, 3a and 4a). Studies were conducted to determine if this trend truly represents the presence of less QDs at greater depths or if it reflects an experimental artifact when imaging deep into tissue. We prepared two *ex vivo* human skin samples in which a high and more homogeneous QD presence was introduced by either QD injection or solution incubation (Supplementary Figure S5a). Image z-stacks were obtained in tissue regions with consistent high QD levels and quantified using ImageJ as described above. Results (Supplementary Figure S5c) show similar intensity profile decays after a depth of 10–15 μm indicating that epidermal light scattering and/or absorption limit the power of the excitation laser and/or the intensity of the QD fluorescence signal collected from deep tissue layers. Nonetheless, the significant differences observed in comparing vehicle group averages are meaningful and valid since these differences occur in the queryable, more superficial layers of skin. The instrumentation imaging parameters were kept constant for all experiments conducted over many days using different donor tissues and different QD batches to ensure accurate comparisons.

In the above section, we showed powerful data indicating the transient effect that tissue processing has on skin barrier function as well as the effects of vehicle composition on QD stratum corneum penetration. Resting human skin (24 h) prior to QD exposure resulted in similar penetration levels to that measured in mouse skin using the petri dish model. However, the inherent architectural and epidermal thickness differences between mouse (~30 μm) and human (~100 μm) skin could affect QD epidermal transit time [12]. To examine the kinetics of QD penetration we conducted a series of parallel experiments using the classic Franz diffusion cell method and compared results to the petri dish exposure model. Eucerin smoothing lotion was the vehicle used in this study. The total fluorescence signal in *ex vivo* mouse skin was integrated from 0 to 40 μm at 3, 6 and 24 h using the petri dish exposure protocol and results were compared to those obtained using the standard Franz

diffusion cell method (Supplementary Figures S6 and S7). We observed that the mouse skin placed in the Franz chamber appeared swollen after 24 h, whereas no gross physical changes were obvious in the mouse skin treated using the petri dish protocol (Supplementary Figures S1 and S8). We quantified the epidermal thickness in the sections of mouse skin that was exposed to the Eucerin Smoothing lotion and GSH QDs for a 24 h duration using the two exposure protocols. A significant difference in the epidermal thickness was observed between the two protocols ($p < 0.05$) (Supplementary Figure S8). Epidermal thickness increase likely results from tissue over-hydration that results from the dermis being in constant contact with the aqueous media reservoir in the Franz cell for 24 h [47–51]. CLSM results showed a higher presence of QDs in the mouse skin at the end of 6 and 24 h using the petri dish exposure protocol compared to the Franz diffusion cell (Figure 6). No significant differences were observed in QD presence at 3 h between the two protocols. Interestingly, at 24 h a significant ($p = 0.01$) decrease in total QD presence in mouse skin was observed compared to the 3 h time point using the Franz chamber method. Though we did not quantify the QD presence in the receiving fluid, based on literature it is expected to be very low and the source of QD on the skin surface was not depleted. Hence, the 24 h result can be attributed to the tissue swelling response that likely dilutes the QD presence within the skin that is imaged (0–40 μm) and/or facilitates a faster QD transit through the skin region that is imaged. These data highlight the impact that the experimental protocol can have on results from which conclusions may be drawn.

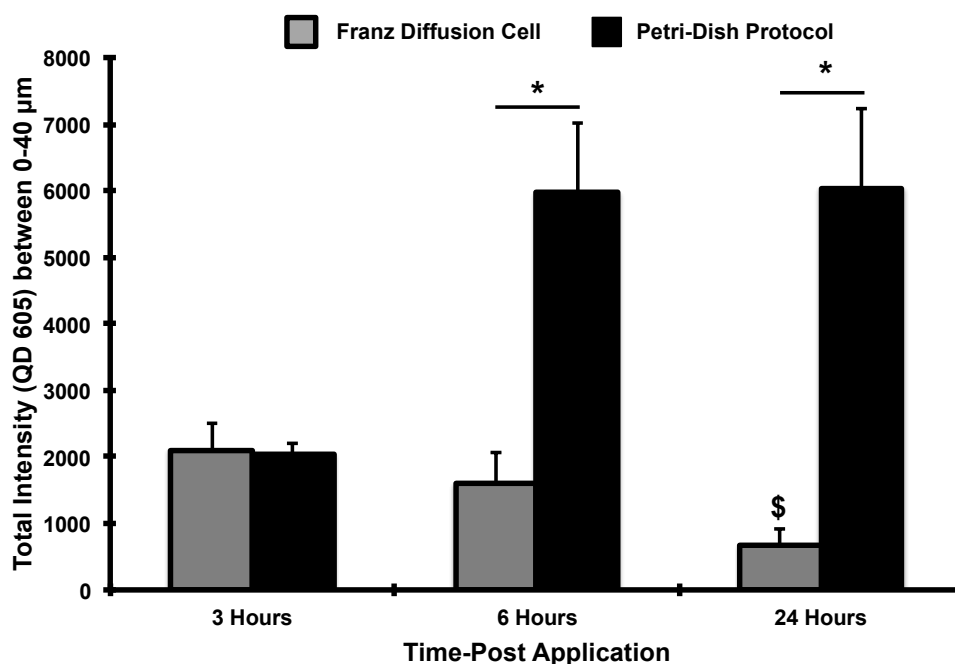


Figure 6. QDs penetrate faster through *ex vivo* mouse skin in the Franz Diffusion Chamber as compared to the petri-dish protocol. The total QD fluorescence signal integrated from 0 to 40 μm was used to quantify the differences in QD epidermal presence in *ex vivo* mouse skin at 3, 6 and 24 h using the petri-dish and Franz cell protocol. A higher presence of QDs was observed in the skin at the end of 6 and 24 h using the petri-dish protocol compared to the Franz cell. A significant decrease in QD presence was observed at 24 h compared to the 3-h time point using the Franz cell; mean \pm SEM ($N = 4$, $n = 3$). * $p < 0.05$ (Inter-group analysis), \$ $p < 0.05$ (3 h vs. 24 h time point Franz cell group).

Eucerin smoothing lotion, glycerol and water vehicles were also used to test QD penetration through human skin (rested) using the Franz diffusion cell and results were compared to the petri dish protocol. Similar penetration levels were observed between the two QD exposure methods for the Eucerin smoothing lotion and water (Supplementary Data Figure S9). However, the glycerol vehicle

showed a 1.7 fold higher QD presence using the petri dish method compared to the Franz cell which may be attributed to its hygroscopic nature combined with tissue swelling.

In summary, the two main objectives of this work were to examine the effect that common commercial skin care lotions may have on the penetration of QD NP in skin and to quantify penetration differences between fresh *ex vivo* human and fresh *ex vivo* hairless mouse skin. In the process, we discovered that the QD skin exposure model (petri dish *vs.* Franz cell), QD exposure time and the processing of *ex vivo* human skin can markedly affect penetration results. Our studies indicate that Eucerin smoothing lotion and glycerol can enhance QD penetration in both *ex vivo* mouse and *ex vivo* human skin models as compared to all the other vehicles investigated. Although all the Eucerin products from Beiersdorf Inc. used in this study contain alpha hydroxyl acids (AHAs), the smoothing lotion is enriched in both AHAs and urea (Supplementary Data Table S1). AHAs are commonly formulated in cosmetic exfoliants, moisturizers and emollients [52,53]. AHAs reduce corneocyte adhesion in the stratum corneum, which alters the skin barrier and consequently enhances the percutaneous absorption of topically applied chemicals [54]. Kraeling and Bronaugh showed that treatment of skin with glycolic acid caused a two-fold increase in the permeability of titrated water [52]. Similarly, urea acts as a penetration enhancer by increasing the hydrolytic content of the stratum corneum, which improves diffusion of topically applied compounds [55]. We did not, however, observe any significant differences in the glycerol treatment group between freshly processed skin and rested (24 h) human skin. Glycerol is also formulated into many commercial lotions for its hygroscopic property, which facilitates skin hydration [43]. However, studies report that applying a high glycerol concentration (>20%–35%) can alter the organization of the intracellular lipids in the stratum corneum causing swelling, water accumulation and a barrier defect [56,57]. This is likely the reason why we did not observe any significant differences in the glycerol treatment group between freshly processed and rested (24 h) human skin (Figure 4b).

Our results employing the Franz diffusion cell exposure protocol suggest an overall lower presence of QDs in both mouse and human skin compared to the petri dish protocol. We attribute this to skin over-hydration that occurs because the dermis is in continuous contact with a circulating media reservoir whereas in the petri dish protocol the dermis is in contact with gauze sheet wetted with media such that overt swelling is not observed. The environment of Franz cell may alter QD presence in the CSLM detection field of view due swelling and the continuously changing concentration gradient. Although the Franz diffusion cell is the accepted industrial and research standard for drug permeation studies it is typically used to quantify the presence of a substance in the receiving chamber. Here, we focused on quantifying QD presence retained in the skin epidermis using CSLM, which is likely impacted by the skin hydration level and dependent on the protocol used.

In comparing the QD penetration between human and mouse skin, we initially measured a substantially higher presence in human skin (Figures 2 and 3), which was unexpected considering the architectural differences between (mouse skin epidermis ~30 μm , human skin epidermis ~100 μm). However, as is common in the literature, we processed *ex vivo* human skin to remove fat prior to use [58]. Resting processed human skin 24 h prior to QD exposure reduced the penetration levels. This finding emphasizes the care that must be taken when using viable skin tissue models for barrier penetration studies. Excised human skin is often stored for a period of 24 h to several weeks under varying temperatures ranging from 4 $^{\circ}\text{C}$ to -80°C before it is used for NP penetration studies by different groups. It is important to note that skin handling, storage, and processing parameters may alter the results obtained [11,16,59,60]. Pentland *et al.* demonstrated that skin trauma induced during subcutaneous fat removal causes mast cell degranulation and increases tissue vascularity [42]. Resting the skin for 24 h post-injury in media allows the skin to heal and refill the histamine stores. In our experimental set-up it is quite possible that both the freshly excised skin (after fat removal) and rested skin show active absorption of QDs, the former higher than the latter which we attribute to skin stress. We demonstrated that QD penetration through rested human skin decreased to levels that measured in mouse skin (Eucerin smoothing lotion and water test groups) that was not subjected to the fat removal

process thereby confirming that the C57BL/6 hairless mouse skin is a useful model for investigating NP skin penetration.

CLSM is an advanced imaging technique employed by various groups to quantify NP penetration through skin [6,61]. This technique allows a three-dimensional reconstruction of the images of the image z-stacks taken. We performed this function (0–40 μm depth) on the vehicle study results and showed that QDs appear to enter the epidermis through high fluency points across the stratum corneum [20]. These may be regions with defects, hair follicles or lacunar pathways (~48 nm diameter, 0.44% presence) in healthy skin [44]. In this work we did not seek to quantify the level of QD penetration relative to the dose applied but it is significant to point out the presence of QDs in the viable epidermis of both mouse and human skin was abundant and no intentional efforts were made to create defects in the stratum corneum barrier through use of physical means (tape strip, dermabrasion, mechanical massage) and the QD lotions were applied with minimal mechanical force exerted to skin. *In vivo* studies designed to quantify the penetration and systemic distribution of QDs that penetrate hairless mouse skin are ongoing.

4. Conclusions

In conclusion our results suggest that certain ingredients (e.g., urea, glycerol, AHAs) found in common commercial skin care lotions can enhance NP penetration. However, it is also possible that the agglomeration state of the QDs mixed in the different application vehicles could affect QD skin penetration. We show using CLSM that no significant differences were observed in overall QD skin penetration levels in fresh *ex vivo* mouse and rested *ex vivo* human skin models using Eucerin smoothing lotion and water vehicles. Processing viable human skin to remove subcutaneous fat and to thin the dermis introduces a transient barrier defect, due in part to the release of histamine stores that can enhance QD penetration. Therefore, it is necessary to rest processed human skin for 24 h prior to NP application. Furthermore, we show that the NP exposure protocol (petri dish *vs.* Franz diffusion cell) affects the magnitude of the QD presence measured in the epidermis and the conclusions that maybe drawn regarding skin penetration. Although this comparison study investigates only C57BL/6 hairless mouse and human skin, it suggests that contrary views regarding the ability of NPs to penetrate skin may simply reflect the wide range of NP types, NP exposure protocols, skin models and skin processing techniques used.

Supplementary Materials: The following are available online at <http://www.mdpi.com/2079-9284/3/1/6/s1>, Table S1, Figures S1–S9.

Acknowledgments: This work was funded by the National Institutes of Health (NIH 1R01ES021492). We thank the Department of Pathology at the University of Rochester Medical Center (URMC) for providing human skin samples for the study. We also thank Maria Jepson and Paivi Jordan at the URMC Confocal Imaging Core for their support.

Author Contributions: Lisa DeLouise and Samreen Jatana conceived the idea; Lisa DeLouise, Samreen Jatana and Alice Pentland designed the experiments; Samreen Jatana and Linda Callahan performed the experiments; Samreen Jatana analyzed the data; Samreen Jatana and Lisa DeLouise wrote the paper.

Conflicts of Interest: The authors state no conflict of interest.

References

1. Praetorius, A.; Scheringer, M.; Hungerbühler, K. Development of environmental fate models for engineered nanoparticles—A case study of TiO₂ nanoparticles in the rhine river. *Environ. Sci. Technol.* **2012**, *46*, 6705–6713. [[CrossRef](#)] [[PubMed](#)]
2. Jatana, S.; DeLouise, L.A. UVR and nanotechnology skin safety. *WIREs Nanomed. Nanobiotechnol.* **2013**, *6*, 61–79. [[CrossRef](#)] [[PubMed](#)]
3. Holsapple, M.P.; Farland, W.H.; Landry, T.D.; Monteiro-Riviere, N.A.; Carter, J.M.; Walker, N.J.; Thomas, K.V. Research strategies for safety evaluation of nanomaterials, part II: Toxicological and safety evaluation of nanomaterials, current challenges and data needs. *Toxicol. Sci.* **2005**, *88*, 12–17. [[CrossRef](#)] [[PubMed](#)]

4. DeLouise, L.A. Applications of nanotechnology in dermatology. *J. Investig. Dermatol.* **2012**, *132*, 964–975. [[CrossRef](#)] [[PubMed](#)]
5. Schneider, M.; Stracke, F.; Hansen, S.; Schaefer, U.F. Nanoparticles and their interactions with the dermal barrier. *Dermatoendocrinol* **2009**, *1*, 197–206. [[CrossRef](#)] [[PubMed](#)]
6. Prow, T.W.; Monteiro-Riviere, N.A.; Inman, A.O.; Grice, J.E.; Chen, X.; Zhao, X.; Sanchez, W.H.; Gierden, A.; Kendall, M.A.; Zvyagin, A.V.; *et al.* Quantum dot penetration into viable human skin. *Nanotoxicology* **2012**, *6*, 173–185. [[CrossRef](#)] [[PubMed](#)]
7. Crosera, M.; Bovenzi, M.; Maina, G.; Adami, G.; Zanette, C.; Florio, C.; Filon Larese, F. Nanoparticle dermal absorption and toxicity: A review of the literature. *Int. Arch. Occup. Environ. Health* **2009**, *82*, 1043–1055. [[CrossRef](#)] [[PubMed](#)]
8. Zhang, L.W.; Yu, W.W.; Colvin, V.L.; Monteiro-Riviere, N.A. Biological interactions of quantum dot nanoparticles in skin and in human epidermal keratinocytes. *Toxicol. Appl. Pharmacol.* **2008**, *228*, 200–211. [[CrossRef](#)] [[PubMed](#)]
9. Schulz, J.; Hohenberg, H.; Pflucker, F.; Gartner, E.; Will, T.; Pfeiffer, S.; Wepf, R.; Wendel, V.; Gers-Barlag, H.; Wittern, K.P. Distribution of sunscreens on skin. *Adv. Drug Deliv. Rev.* **2002**, *54* (Suppl. 1), S157–S163. [[CrossRef](#)]
10. Burnett, M.E.; Wang, S.Q. Current sunscreen controversies: A critical review. *Photodermatol. Photoimmunol. Photomed.* **2011**, *27*, 58–67. [[CrossRef](#)] [[PubMed](#)]
11. Baroli, B.; Ennas, M.G.; Loffredo, F.; Isola, M.; Pinna, R.; Lopez-Quintela, M.A. Penetration of metallic nanoparticles in human full-thickness skin. *J. Investig. Dermatol.* **2007**, *127*, 1701–1712. [[CrossRef](#)] [[PubMed](#)]
12. Baroli, B. Penetration of nanoparticles and nanomaterials in the skin: Fiction or reality? *J. Pharm. Sci.* **2010**, *99*, 21–50. [[CrossRef](#)] [[PubMed](#)]
13. Gopee, N.V.; Roberts, D.W.; Webb, P.; Cozart, C.R.; Siitonen, P.H.; Latendresse, J.R.; Warbitton, A.R.; Yu, W.W.; Colvin, V.L.; Walker, N.J.; *et al.* Quantitative determination of skin penetration of PEG-coated cadmium quantum dots in dermabraded but not intact SKH-1 hairless mouse skin. *Toxicol. Sci.* **2009**, *111*, 37–48. [[CrossRef](#)] [[PubMed](#)]
14. Desai, P.; Patlolla, R.R.; Singh, M. Interaction of nanoparticles and cell-penetrating peptides with skin for transdermal drug delivery. *Mol. Membr. Biol.* **2010**, *27*, 247–259. [[CrossRef](#)] [[PubMed](#)]
15. Labouta, H.I.; Hampel, M.; Thude, S.; Reutlinger, K.; Kostka, K.H.; Schneider, M. Depth profiling of gold nanoparticles and characterization of point spread functions in reconstructed and human skin using multiphoton microscopy. *J. Biophotonics* **2012**, *5*, 85–96. [[CrossRef](#)] [[PubMed](#)]
16. Labouta, H.I.; El-Khordagui, L.K.; Kraus, T.; Schneider, M. Mechanism and determinants of nanoparticle penetration through human skin. *Nanoscale* **2011**, *3*, 4989–4999. [[CrossRef](#)] [[PubMed](#)]
17. Gratieri, T.; Schaefer, U.F.; Jing, L.; Gao, M.; Kostka, K.H.; Lopez, R.F.; Schneider, M. Penetration of quantum dot particles through human skin. *J. Biomed. Nanotechnol.* **2010**, *6*, 586–595. [[CrossRef](#)] [[PubMed](#)]
18. Ravichandran, S.; Mortensen, L.J.; DeLouise, L.A. Quantification of human skin barrier function and susceptibility to quantum dot skin penetration. *Nanotoxicology* **2011**, *5*, 675–686. [[CrossRef](#)] [[PubMed](#)]
19. Mortensen, L.J.; Oberdorster, G.; Pentland, A.P.; Delouise, L.A. *In vivo* skin penetration of quantum dot nanoparticles in the murine model: The effect of UVR. *Nano Lett.* **2008**, *8*, 2779–2787. [[CrossRef](#)] [[PubMed](#)]
20. Mortensen, L.J.; Jatana, S.; Gelein, R.; de Benedetto, A.; de Mesy Bentley, K.L.; Beck, L.A.; Elder, A.; Delouise, L.A. Quantification of quantum dot murine skin penetration with UVR barrier impairment. *Nanotoxicology* **2013**, *7*, 1386–1398. [[CrossRef](#)] [[PubMed](#)]
21. Riviere, N.A.M.; Zhang, L.W. Assessment of quantum dot penetration into skin in different species under different mechanical actions. In *Nanomaterials: Risks and Benefits*; Springer Science + Business Media B.V.: Berlin, Heidelberg, Germany, 2009; pp. 43–52.
22. Wu, X.; Price, G.J.; Guy, R.H. Disposition of nanoparticles and an associated lipophilic permeant following topical application to the skin. *Mol. Pharm.* **2009**, *6*, 1441–1448. [[CrossRef](#)] [[PubMed](#)]
23. Wu, X.; Landfester, K.; Musyanovych, A.; Guy, R.H. Disposition of charged nanoparticles after their topical application to the skin. *Skin Pharmacol. Physiol.* **2010**, *23*, 117–123. [[CrossRef](#)] [[PubMed](#)]
24. Abdel-Mottaleb, M.M.A.; Moulari, B.; Beduneau, A.; Pellequer, Y.; Lamprecht, A. Nanoparticles enhance therapeutic outcome in inflamed skin therapy. *Eur. J. Pharm. Biopharm.* **2012**, *82*, 151–157. [[CrossRef](#)] [[PubMed](#)]

25. Mak, W.C.; Richter, H.; Patzelt, A.; Sterry, W.; Lai, K.K.; Renneberg, R.; Lademann, J. Drug delivery into the skin by degradable particles. *Eur. J. Pharm. Biopharm.* **2011**, *79*, 23–27. [[CrossRef](#)] [[PubMed](#)]
26. Lademann, J.; Richter, H.; Meinke, M.C.; Lange-Asschenfeldt, B.; Antoniou, C.; Mak, W.C.; Renneberg, R.; Sterry, W.; Patzelt, A. Drug delivery with topically applied nanoparticles: Science fiction or reality? *Skin Pharmacol. Physiol.* **2013**, *26*, 227–233. [[CrossRef](#)] [[PubMed](#)]
27. Patzelt, A.; Lademann, J. Drug delivery to hair follicles. *Expert Opin. Drug Deliv.* **2013**, *10*, 787–797. [[CrossRef](#)] [[PubMed](#)]
28. Ostrowski, A.; Nordmeyer, D.; Boreham, A.; Brodewolf, R.; Mundhenk, L.; Fluhr, J.W.; Lademann, J.; Graf, C.; Ruhl, E.; Alexiev, U.; *et al.* Skin barrier disruptions in tape stripped and allergic dermatitis models have no effect on dermal penetration and systemic distribution of ahaps-functionalized silica nanoparticles. *Nanomedicine* **2014**, *10*, 1571–1581. [[CrossRef](#)] [[PubMed](#)]
29. Morganti, P.; Morganti, G. Chitin nanofibrils for advanced cosmeceuticals. *Clin. Dermatol.* **2008**, *26*, 334–340. [[CrossRef](#)] [[PubMed](#)]
30. Morganti, P. Use and potential of nanotechnology in cosmetic dermatology. *Clin. Cosmet. Investig. Dermatol.* **2010**, *3*, 5–13. [[CrossRef](#)] [[PubMed](#)]
31. Patzelt, A.; Richter, H.; Knorr, F.; Schafer, U.; Lehr, C.M.; Dahne, L.; Sterry, W.; Lademann, J. Selective follicular targeting by modification of the particle sizes. *J. Controll. Release* **2011**, *150*, 45–48. [[CrossRef](#)] [[PubMed](#)]
32. Patzelt, A.; Richter, H.; Dahne, L.; Walden, P.; Wiesmuller, K.H.; Wank, U.; Sterry, W.; Lademann, J. Influence of the vehicle on the penetration of particles into hair follicles. *Pharmaceutics* **2011**, *3*, 307–314. [[CrossRef](#)] [[PubMed](#)]
33. Zheng, D.; Giljohann, D.A.; Chen, D.L.; Massich, M.D.; Wang, X.Q.; Iordanov, H.; Mirkin, C.A.; Paller, A.S. Topical delivery of siRNA-based spherical nucleic acid nanoparticle conjugates for gene regulation. *Proc. Natl. Acad. Sci. USA* **2012**, *109*, 11975–11980. [[CrossRef](#)] [[PubMed](#)]
34. Wang, X.; Xu, W.; Mohapatra, S.; Kong, X.; Li, X.; Lockey, R.F.; Mohapatra, S.S. Prevention of airway inflammation with topical cream containing imiquimod and small interfering RNA for natriuretic peptide receptor. *Genet. Vaccines Ther.* **2008**, *6*. [[CrossRef](#)] [[PubMed](#)]
35. Monteiro-Riviere, N.A.; Wiench, K.; Landsiedel, R.; Schulte, S.; Inman, A.O.; Riviere, J.E. Safety evaluation of sunscreen formulations containing titanium dioxide and zinc oxide nanoparticles in UVB sunburned skin: An *in vitro* and *in vivo* study. *Toxicol. Sci.* **2011**, *123*, 264–280. [[CrossRef](#)] [[PubMed](#)]
36. Walters, K.A.; Roberts, M.S. *Dermatological and Transdermal Formulations*; CRC Press: Boca Raton, FL, USA, 2002; Volume 119, p. 574.
37. Sanderson, K. Quantum dots go large. *Nature* **2009**, *459*, 760–761. [[CrossRef](#)] [[PubMed](#)]
38. Jamieson, T.; Bakhshi, R.; Petrova, D.; Pockock, R.; Imani, M.; Seifalian, A.M. Biological applications of quantum dots. *Biomaterials* **2007**, *28*, 4717–4732. [[CrossRef](#)] [[PubMed](#)]
39. Zhang, L.S.W.; Monteiro-Riviere, N.A. Use of confocal microscopy for nanoparticle drug delivery through skin. *J. Biomed. Opt.* **2013**, *18*. [[CrossRef](#)] [[PubMed](#)]
40. Monteiro-Riviere, N.A. Introduction to histological aspects of dermatotoxicology. *Microsc. Res. Tech.* **1997**, *37*, 171. [[CrossRef](#)]
41. Zheng, H.; Mortensen, L.J.; DeLouise, L.A. Thiol antioxidant-functionalized CdSe/ZnS quantum dots: Synthesis, characterization, cytotoxicity. *J. Biomed. Nanotechnol.* **2013**, *9*, 382–392. [[CrossRef](#)] [[PubMed](#)]
42. Pentland, A.P.; Mahoney, M.; Jacobs, S.C.; Holtzman, M.J. Enhanced prostaglandin synthesis after ultraviolet injury is mediated by endogenous histamine stimulation. A mechanism for irradiation erythema. *J. Clin. Investig.* **1990**, *86*, 566–574. [[CrossRef](#)] [[PubMed](#)]
43. Fluhr, J.W.; Darlenski, R.; Surber, C. Glycerol and the skin: Holistic approach to its origin and functions. *Br. J. Dermatol.* **2008**, *159*, 23–34. [[CrossRef](#)] [[PubMed](#)]
44. Paliwal, S.; Menon, G.K.; Mitragotri, S. Low-frequency sonophoresis: Ultrastructural basis for stratum corneum permeability assessed using quantum dots. *J. Investig. Dermatol.* **2006**, *126*, 1095–1101. [[CrossRef](#)] [[PubMed](#)]
45. Abdel-Mottaleb, M.M.A.; Moulari, B.; Beduneau, A.; Pellequer, Y.; Lamprecht, A. Surface-charge-dependent nanoparticles accumulation in inflamed skin. *J. Pharm. Sci.* **2012**, *101*, 4231–4239. [[CrossRef](#)] [[PubMed](#)]
46. Batt, M.D.; Davis, W.B.; Fairhurst, E.; Gerrard, W.A.; Ridge, B.D. Changes in the physical-properties of the stratum-corneum following treatment with glycerol. *J. Soc. Cosmet. Chem.* **1988**, *39*, 367–381.

47. Aguzzi, C.; Rossi, S.; Bagnasco, M.; Lanata, L.; Sandri, G.; Bona, F.; Ferrari, F.; Bonferoni, M.C.; Caramella, C. Penetration and distribution of thiocolchicoside through human skin: Comparison between a commercial foam (miotens) and a drug solution. *AAPS PharmSciTech* **2008**, *9*, 1185–1190. [[CrossRef](#)] [[PubMed](#)]
48. Van Kuijk-Meuwissen, M.E.; Junginger, H.E.; Bouwstra, J.A. Interactions between liposomes and human skin *in vitro*, a confocal laser scanning microscopy study. *Biochim. Biophys. Acta* **1998**, *1371*, 31–39. [[CrossRef](#)]
49. Wagner, H.; Kostka, K.H.; Lehr, C.M.; Schaefer, U.F. Human skin penetration of flufenamic acid: *In vivo/in vitro* correlation (deeper skin layers) for skin samples from the same subject. *J. Investig. Dermatol.* **2002**, *118*, 540–544. [[CrossRef](#)] [[PubMed](#)]
50. Neelissen, J.A.; Arth, C.; Schrijvers, A.H.; Junginger, H.E.; Bodde, H.E. Validation of freeze-drying to visualize percutaneous 3h-estradiol transport: The influence of skin hydration on the efficacy of the method. *Skin Pharmacol. Appl. Skin Physiol.* **1998**, *11*, 11–22. [[CrossRef](#)] [[PubMed](#)]
51. Levintova, Y.; Plakogiannis, F.M.; Bellantone, R.A. An improved *in vitro* method for measuring skin permeability that controls excess hydration of skin using modified franz diffusion cells. *Int. J. Pharm.* **2011**, *419*, 96–106. [[CrossRef](#)] [[PubMed](#)]
52. Kraeling, M.E.K.; Bronaugh, R.L. *In vitro* percutaneous absorption of alpha hydroxy acids in human skin. *J. Soc. Cosmet. Chem.* **1997**, *48*, 187–197.
53. Hood, H.L.; Kraeling, M.E.K.; Robl, M.G.; Bronaugh, R.L. The effects of an alpha hydroxy acid (glycolic acid) on hairless guinea pig skin. *J. Soc. Cosmet. Chem.* **1997**, *48*, 53–55. [[CrossRef](#)]
54. Copovi, A.; Diez-Sales, O.; Herraes-Dominguez, J.V.; Herraes-Dominguez, M. Enhancing effect of alpha-hydroxyacids on “*in vitro*” permeation across the human skin of compounds with different lipophilicity. *Int. J. Pharm.* **2006**, *314*, 31–36. [[CrossRef](#)] [[PubMed](#)]
55. Trommer, H.; Neubert, R.H. Overcoming the stratum corneum: The modulation of skin penetration. A review. *Skin Pharmacol. Physiol.* **2006**, *19*, 106–121. [[CrossRef](#)] [[PubMed](#)]
56. Caussin, J.; Gooris, G.S.; Bouwstra, J.A. Ftir studies show lipophilic moisturizers to interact with stratum corneum lipids, rendering the more densely packed. *Biochim. Biophys. Acta* **2008**, *1778*, 1517–1524. [[CrossRef](#)] [[PubMed](#)]
57. Caussin, J.; Gooris, G.S.; Janssens, M.; Bouwstra, J.A. Lipid organization in human and porcine stratum corneum differs widely, while lipid mixtures with porcine ceramides model human stratum corneum lipid organization very closely. *Biochim. Biophys. Acta* **2008**, *1778*, 1472–1482. [[CrossRef](#)] [[PubMed](#)]
58. Larese, F.F.; D’Agostin, F.; Crosera, M.; Adami, G.; Renzi, N.; Bovenzi, M.; Maina, G. Human skin penetration of silver nanoparticles through intact and damaged skin. *Toxicology* **2009**, *255*, 33–37. [[CrossRef](#)] [[PubMed](#)]
59. Liu, D.C.; Raphael, A.P.; Sundh, D.; Grice, J.E.; Soyer, H.P.; Roberts, M.S.; Prow, T.W. The human stratum corneum prevents small gold nanoparticle penetration and their potential toxic metabolic consequences. *J. Nanomater.* **2012**, *2012*. [[CrossRef](#)]
60. Filon, F.L.; Crosera, M.; Adami, G.; Bovenzi, M.; Rossi, F.; Maina, G. Human skin penetration of gold nanoparticles through intact and damaged skin. *Nanotoxicology* **2011**, *5*, 493–501. [[CrossRef](#)] [[PubMed](#)]
61. Alvarez-Roman, R.; Naik, A.; Kalia, Y.N.; Fessi, H.; Guy, R.H. Visualization of skin penetration using confocal laser scanning microscopy. *Eur. J. Pharm. Biopharm.* **2004**, *58*, 301–316. [[CrossRef](#)] [[PubMed](#)]



© 2016 by the authors; licensee MDPI, Basel, Switzerland. This article is an open access article distributed under the terms and conditions of the Creative Commons by Attribution (CC-BY) license (<http://creativecommons.org/licenses/by/4.0/>).